

A dynamic subgrid-scale eddy viscosity model

By Massimo Germano,¹ Ugo Piomelli,²
Parviz Moin³ AND William H. Cabot³

One major drawback of the eddy viscosity subgrid-scale stress models used in large-eddy simulations is their inability to represent correctly with a single universal constant different turbulent fields in rotating or sheared flows, near solid walls, or in transitional regimes. In the present work a new eddy viscosity model is presented which alleviates many of these drawbacks. The model coefficient is computed dynamically as the calculation progresses rather than input *a priori*. The model is based on an algebraic identity (Germano 1990) between the subgrid-scale stresses at two different filtered levels and the resolved turbulent stresses. The subgrid-scale stresses obtained using the proposed model vanish in laminar flow and at a solid boundary, and have the correct asymptotic behavior in the near-wall region of a turbulent boundary layer. The results of large-eddy simulations of transitional and turbulent channel flow that use the proposed model are in good agreement with the direct simulation data.

1. Introduction

In large-eddy simulations (LES) the effect of the large scales is directly computed, and only the small subgrid scales are modeled. Since small scales tend to be more isotropic than the large ones, it should be possible to parameterize them using simpler and more universal models than standard Reynolds stress models. Thus, most subgrid-scale (SGS) stress models are based on an eddy viscosity assumption. In the most commonly used model, due to Smagorinsky (1963), the eddy viscosity ν_T is obtained by assuming that the small scales are in equilibrium, so that energy production and dissipation are in balance. This yields an expression of the form

$$\nu_T = (C_S \Delta)^2 |\bar{S}|, \quad (1)$$

where Δ is the filter width (which, unless otherwise noted, is assumed to be equal to the grid size), C_S is the Smagorinsky constant, $|\bar{S}| = (2\bar{S}_{ij}\bar{S}_{ij})^{1/2}$ is the magnitude of large-scale strain rate tensor

$$\bar{S}_{ij} = \frac{1}{2} \left(\frac{\partial \bar{u}_i}{\partial x_j} + \frac{\partial \bar{u}_j}{\partial x_i} \right), \quad (2)$$

¹ Politecnico di Torino, Italy

² University of Maryland

³ Center for Turbulence Research

and \bar{u}_i is the large-scale velocity.

Lilly (1966) determined that, for homogeneous isotropic turbulence with cutoff in the inertial subrange, $C_S \approx 0.17$. In the presence of mean shear, however, this value was found to cause excessive damping of large-scale fluctuations, and in his simulation of turbulent channel flow, Deardorff (1971) used $C_S = 0.094$. *A priori* tests by McMillan, Ferziger & Rogallo (1980) on homogeneous turbulence confirmed that C_S decreases with increasing strain rate. Mason & Callen (1986), however, found that the value $C_S = 0.2$ gave good results if the grid resolution was sufficiently fine, and concluded that values of C_S lower than 0.2 are required if the numerical resolution is insufficient. Their results, however, were not confirmed by Piomelli, Moin & Ferziger (1988), who found the optimum value of C_S to be around 0.1 even with meshes much finer than those used by Mason & Callen (1986).

Additional modifications to the Smagorinsky model were made in the near-wall region of plane channels to force the subgrid-scale stresses to vanish at the solid boundary. Moin & Kim (1982), for example, used damping functions to account for near-wall effects. Piomelli *et al.* (1988) chose the damping function to ensure the proper asymptotic behavior for the SGS shear stresses near the wall, but found little difference with the results obtained with the standard Van Driest (1956) damping used by Moin & Kim (1982) and others.

Yakhot *et al.* (1989) used a subgrid-scale model based on the Renormalization Group theory of Yakhot & Orszag (1986) in the large-eddy simulation of channel flow. Although the stresses predicted by the model in its original formulation go to zero without requiring any damping function, Yakhot *et al.* (1989) included an *ad hoc* factor to take into account the anisotropy of the small-scales in the near-wall region. The asymptotic behavior of the stresses predicted by this model depends on the grid distribution in the wall-normal direction; for the grids commonly used, an incorrect asymptotic behavior is obtained.

Large-eddy simulations of transition in boundary layers (Piomelli *et al.* 1990a) and plane channel (Piomelli & Zang 1990b) show that during the early stages of transition the Smagorinsky model predicts excessive damping of the resolved structures, leading to incorrect growth rates of the initial perturbations. To overcome this difficulty they introduced additional empiricism in the form of an intermittency function which modified the Smagorinsky constant by effectively setting it to zero during the linear and early nonlinear stages of transition.

This brief survey of the existing literature indicates that, although modifications of the Smagorinsky model have been successfully applied to the LES of transitional and turbulent flows, it is not possible to model effectively with a single, universal constant the variety of phenomena present in the flows examined. The *ad hoc* manner in which the SGS eddy viscosity has been extrapolated to the wall is far from desirable. In addition the Smagorinsky model cannot account for energy flow from small scales to large scales (backscatter), which can be significant (Piomelli *et al.* 1990c).

In this work a new, dynamic SGS stress model is proposed that attempts to overcome these deficiencies by locally calculating the eddy viscosity coefficient to

reflect closely the state of the flow. This is done by sampling the smallest resolved scales and using this information to model the subgrid scales. The model presented here requires a single input parameter and exhibits the proper asymptotic behavior near solid boundaries or in laminar flow without requiring damping or intermittency functions. The model is also capable of accounting for backscatter.

In the next Section, the model will be presented and its characteristics discussed. The model was tested both *a priori*, taking advantage of existing direct numerical simulation (DNS) databases, and *a posteriori* using the model in an LES calculation. The results of these tests will be discussed in Section 3. Concluding remarks will be made in Section 4.

2. Mathematical formulation

In large-eddy simulation, the large scale quantities are defined by the convolution of the velocity and pressure fields with a filter function. For the purposes of this work we define two filtering operators: one is the *grid* filter, \bar{G} , denoted by an overbar:

$$\bar{f}(\mathbf{x}) = \int f(\mathbf{x}') \bar{G}(\mathbf{x}, \mathbf{x}') d\mathbf{x}', \quad (3)$$

while the other, the *test* filter, \tilde{G} , is denoted by a tilde:

$$\tilde{f}(\mathbf{x}) = \int f(\mathbf{x}') \tilde{G}(\mathbf{x}, \mathbf{x}') d\mathbf{x}'; \quad (4)$$

finally, let $\tilde{\bar{G}} = \bar{G}\tilde{G}$.

By applying the grid filter to the dimensionless continuity and Navier-Stokes equations one obtains the filtered equations of motions

$$\frac{\partial \bar{u}_i}{\partial x_i} = 0, \quad (5)$$

$$\frac{\partial \bar{u}_i}{\partial t} + \frac{\partial}{\partial x_j} (\bar{u}_i \bar{u}_j) = - \frac{\partial \bar{p}}{\partial x_i} - \frac{\partial \tau_{ij}}{\partial x_j} + \frac{1}{Re} \frac{\partial^2 \bar{u}_i}{\partial x_j \partial x_j}. \quad (6)$$

In the following, x or x_1 is the streamwise direction, y or x_2 the wall-normal direction and z or x_3 is the spanwise direction. The effects of the small scales appear in the subgrid-scale stress term

$$\tau_{ij} = \bar{u}_i \bar{u}_j - \bar{u}_i \bar{u}_j, \quad (7)$$

which must be modeled.

Consider now the subgrid-scale stress obtained by applying the test filter to the filtered equations of motion (5) and (6)

$$T_{ij} = \widetilde{\bar{u}_i \bar{u}_j} - \widetilde{\bar{u}_i} \widetilde{\bar{u}_j}, \quad (8)$$

and the resolved turbulent stress \mathcal{L}_{ij} defined as

$$\mathcal{L}_{ij} = \widetilde{\bar{u}_i \bar{u}_j} - \widetilde{\bar{u}_i} \widetilde{\bar{u}_j}. \quad (9)$$

The resolved turbulent stresses are representative of the contribution to the Reynolds stresses by the scales whose length is intermediate between the grid filter width and the test filter width, i.e. the small resolved scales. It is easy to see that these quantities are related by the algebraic relation (Germano 1990)

$$\mathcal{L}_{ij} = T_{ij} - \tilde{\tau}_{ij}, \quad (10)$$

which relates the resolved turbulent stress \mathcal{L}_{ij} , which can be calculated explicitly, to the subgrid-scale stresses at the test and grid levels, T_{ij} and τ_{ij} .

The identity (10) can be exploited to derive more accurate SGS stress models by determining, for example, the value of the Smagorinsky coefficient most appropriate to the instantaneous state of the flow. Assuming that the same functional form can be used to parameterize both T_{ij} and τ_{ij} (the Smagorinsky model, for example), let M_{ij} and m_{ij} be the models for the anisotropic parts of the T_{ij} and τ_{ij} :

$$\tau_{ij} - \frac{\delta_{ij}}{3}\tau_{kk} \simeq m_{ij} = -2C\bar{\Delta}^2|\bar{S}|\bar{S}_{ij}, \quad (11)$$

$$T_{ij} - \frac{\delta_{ij}}{3}T_{kk} \simeq M_{ij} = -2C\tilde{\Delta}^2|\tilde{S}|\tilde{S}_{ij}, \quad (12)$$

where

$$\tilde{S}_{ij} = \frac{1}{2} \left(\frac{\partial \tilde{u}_i}{\partial x_j} + \frac{\partial \tilde{u}_j}{\partial x_i} \right), \quad |\tilde{S}| = \sqrt{2\tilde{S}_{mn}\tilde{S}_{mn}}, \quad (13)$$

$\bar{\Delta}$ is the characteristic filter width associated with \bar{G} , and $\tilde{\Delta}$ is filter width associated with \tilde{G} . Substitution of (11) and (12) into (10) and contracting with \bar{S}_{ij} (or \tilde{S}_{ij}) gives

$$\mathcal{L}_{ij}\bar{S}_{ij} = -2C \left(\tilde{\Delta}^2|\tilde{S}|\tilde{S}_{ij}\bar{S}_{ij} - \bar{\Delta}^2|\bar{S}|\bar{S}_{ij}\bar{S}_{ij} \right), \quad (14)$$

from which $C(x, y, z, t)$ can, apparently, be easily obtained. The quantity in parentheses, however, can become zero which would make C indeterminate or ill-conditioned. *A priori* tests in turbulent channel flow have shown this to be indeed the case. For the channel flow, therefore, it was assumed that C is only a function of y and t . To this end, the average of both sides of (14) is taken over a plane parallel to the wall (indicated by $\langle \cdot \rangle$) to yield

$$C(y, t) = -\frac{1}{2} \frac{\langle \mathcal{L}_{kl}\bar{S}_{kl} \rangle}{\tilde{\Delta}^2 \langle |\tilde{S}|\tilde{S}_{mn}\bar{S}_{mn} \rangle - \bar{\Delta}^2 \langle |\bar{S}|\bar{S}_{pq}\bar{S}_{pq} \rangle}; \quad (15)$$

the new dynamic eddy viscosity subgrid-scale stress model is then given by

$$m_{ij} = \frac{\langle \mathcal{L}_{kl}\bar{S}_{kl} \rangle}{\left(\tilde{\Delta}/\bar{\Delta}\right)^2 \langle |\tilde{S}|\tilde{S}_{mn}\bar{S}_{mn} \rangle - \langle |\bar{S}|\bar{S}_{pq}\bar{S}_{pq} \rangle} |\bar{S}|\bar{S}_{ij}. \quad (16)$$

In more general situations, the plane average should be replaced with appropriate local space and time averages.

A few remarks are in order regarding the properties and the character of the subgrid-scale stress model given by (16). First, the model gives zero SGS stress everywhere \mathcal{L}_{ij} vanishes (as long as the denominator remains finite). Such is the case in laminar flow or at solid boundaries. Furthermore, it is easy to show that in the near-wall region m_{ij} is proportional to the cube of the distance from the wall y_w , regardless of the choice of $\bar{\Delta}$ or $\tilde{\Delta}$. This is the correct asymptotic behavior for the (1,2) component of the subgrid-scale stress tensor, which, in this region, is the most significant one. To the authors' knowledge, this is the only model which satisfies this property without the use of *ad hoc* damping functions. Finally, the use of (16) implies that the modeled subgrid-scale dissipation, $\epsilon_{sgs} = m_{ij}\bar{S}_{ij}$, is proportional to the average dissipation of the resolved turbulent stresses, $\langle \mathcal{L}_{ij}\bar{S}_{ij} \rangle$, which can be either positive or negative. Thus, the model does not rule out backscatter. In the present formulation backscatter is not localized, and may (or may not) occur at every point in a plane; the use of local averaging in (14), however, would allow the model to provide localized backscatter as well.

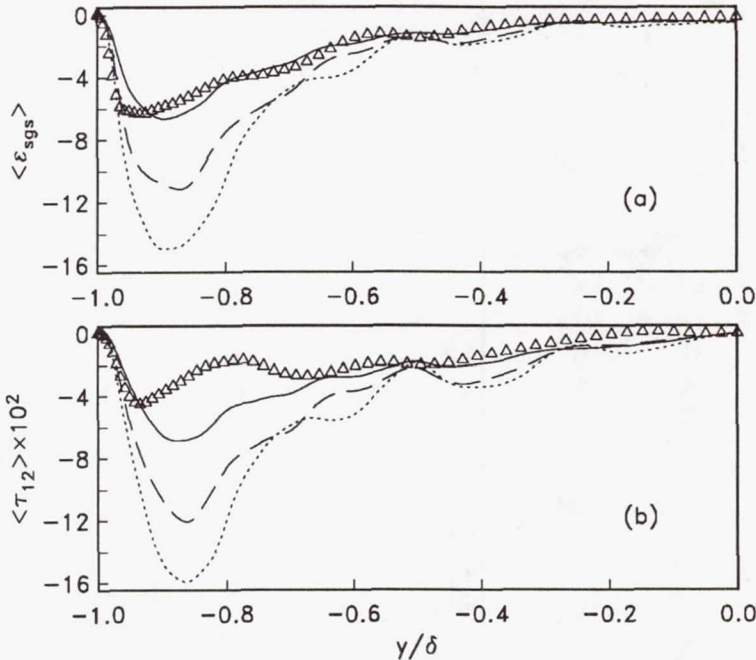
The only adjustable parameter in the model is the ratio $\alpha = \tilde{\Delta}/\bar{\Delta} > 1$. The resolved turbulent stresses calculated using small values of α can be contaminated by numerical errors; on the other hand, large values of α imply that the stresses due to large energy carrying structures are used to determine the contribution of the subgrid scales. If the optimal value of α varies greatly from one flow to another, the applicability of the model is reduced. In the next Section, the optimal value of α obtained from a turbulent channel flow database will be used for the large-eddy simulation of transitional and turbulent channel flow at higher Reynolds numbers to address this issue. Finally, the model (16) implicitly assumes similarity between the SGS stresses at the grid and test levels, which are modeled using the same functional expression, namely, the Smagorinsky model.

3. Results and discussion

A priori tests of the dynamic subgrid-scale stress model (16) were carried out to determine the best choice for α and the accuracy with which the model predicts the SGS stresses and dissipation. The tests were performed using the DNS database of Kim, Moin & Moser (1987) for turbulent channel flow, and that of Zang, Gilbert & Kleiser (1990) for transitional flow. Reynolds numbers are respectively $Re = 3300$ (based on the centerline velocity U_c and channel halfwidth δ) for the turbulent case, and $Re = 8000$ for the transitional case (based on initial centerline velocity and channel halfwidth).

The first task accomplished by these tests was to determine the optimal value of the ratio α . The sharp cutoff filter was applied as both grid and test filter in the streamwise and spanwise directions. No explicit filtering was applied in the wall-normal direction. The length scales were defined as

$$\bar{\Delta}^3 = \bar{\Delta}_1 \bar{\Delta}_2 \bar{\Delta}_3, \quad \tilde{\Delta}^3 = \tilde{\Delta}_1 \tilde{\Delta}_2 \tilde{\Delta}_3, \quad (17)$$



where $\bar{\Delta}_i$ and $\tilde{\bar{\Delta}}_i$ are the filter widths in each coordinate direction associated with \bar{G} and $\tilde{\bar{G}}$ respectively.

The mean subgrid-scale shear stress $\langle \tau \rangle_{12}$ and dissipation $\langle \epsilon_{sgs} \rangle$ are compared with the modeled ones in Figure 1 for various filter widths in the turbulent channel flow case. The choice $\alpha = 2$ was found to yield the best results. With this choice $\bar{\Delta}$ corresponds to a wavenumber in the decaying region of the one-dimensional energy spectrum, while $\tilde{\bar{\Delta}}$ represents a wavenumber in the flat region. In Figure 2, C is plotted as function of the wall coordinate $y^+ = u_\tau y_w / \nu$ [where $u_\tau = (\tau_w / \rho)^{1/2}$ is the friction velocity, τ_w is the wall shear and ρ the fluid density] ; the expected y^{+3} behavior is evident. At the channel center $C \simeq 2.5 \times 10^{-3}$; the square root of this value is about half the commonly used value for the Smagorinsky constant, $C_S = 0.1$. The model was also tested in transitional flow, where the choice $\alpha = 2$ appeared to be the best, at least for the prediction of the subgrid-scale dissipation

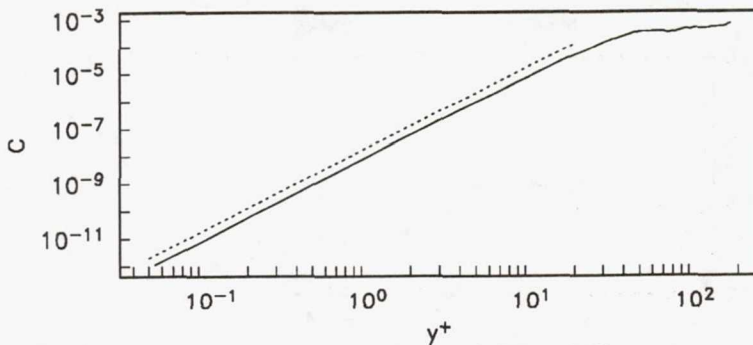


FIGURE 2. Variation of C [defined in Eqn. (16)] with distance from the wall; $Re = 3300$ turbulent channel flow, $\alpha = 2$. — C obtained from DNS (Kim *et al.* 1987); $C \sim y^+^3$.

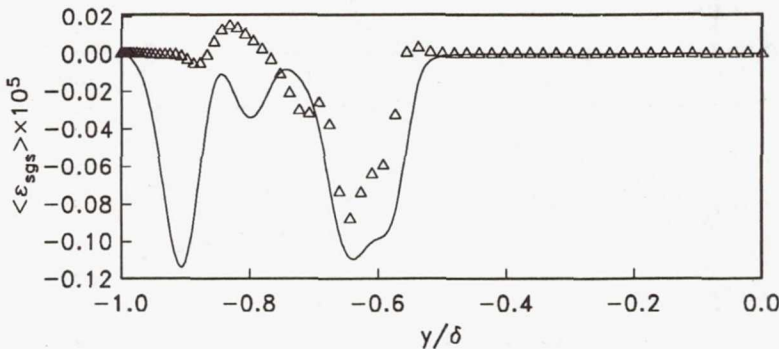


FIGURE 3. Plane-averaged subgrid-scale dissipation $\langle \varepsilon_{sgs} \rangle$; transitional flow, $t = 176$. \triangle exact; — $\alpha = 2$.

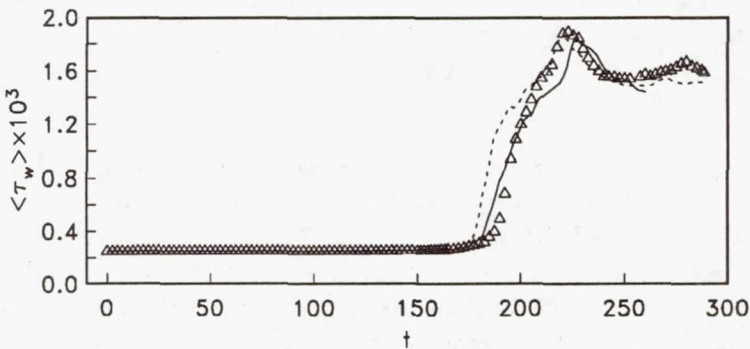


FIGURE 4. Time development of the plane-averaged wall shear stress $\langle \tau_w \rangle$ in $Re = 8000$ transitional channel flow. \triangle DNS (Zang *et al.* 1990); — present results; LES (Piomelli & Zang 1990b).

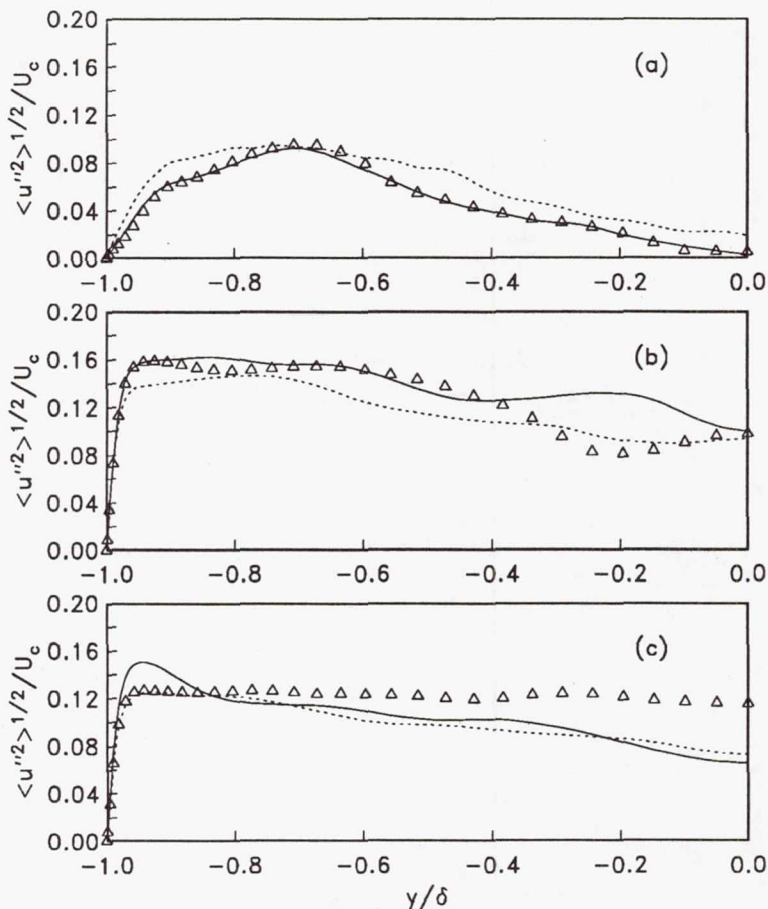


FIGURE 5. Turbulence intensities $\langle u''^2 \rangle^{1/2}$ in transitional channel flow. Δ Filtered DNS (Zang *et al.* 1990); — present calculation; LES results of Piomelli & Zang (1990b). (a) $t = 176$; (b) $t = 200$; (c) $t = 220$.

(Figure 3). The SGS dissipation predicted by the Smagorinsky model, by contrast, is many orders of magnitude larger, and peaks much closer to the wall than the exact one (Piomelli *et al.* 1990a).

To further determine the accuracy of the dynamic SGS model (16), it was also tested *a posteriori* in the LES of transitional and fully developed turbulent channel flow. Initial conditions consisted of the parabolic mean flow, on which a 2D Tollmien-Schlichting (TS) mode of 2% amplitude and a 3D TS mode of 0.02% amplitude were superimposed. The initial conditions and Reynolds number matched those of the direct simulation of Zang, Gilbert & Kleiser (1990). The governing equations (5) and (6) were integrated in time using a pseudo-spectral Fourier-Chebyshev

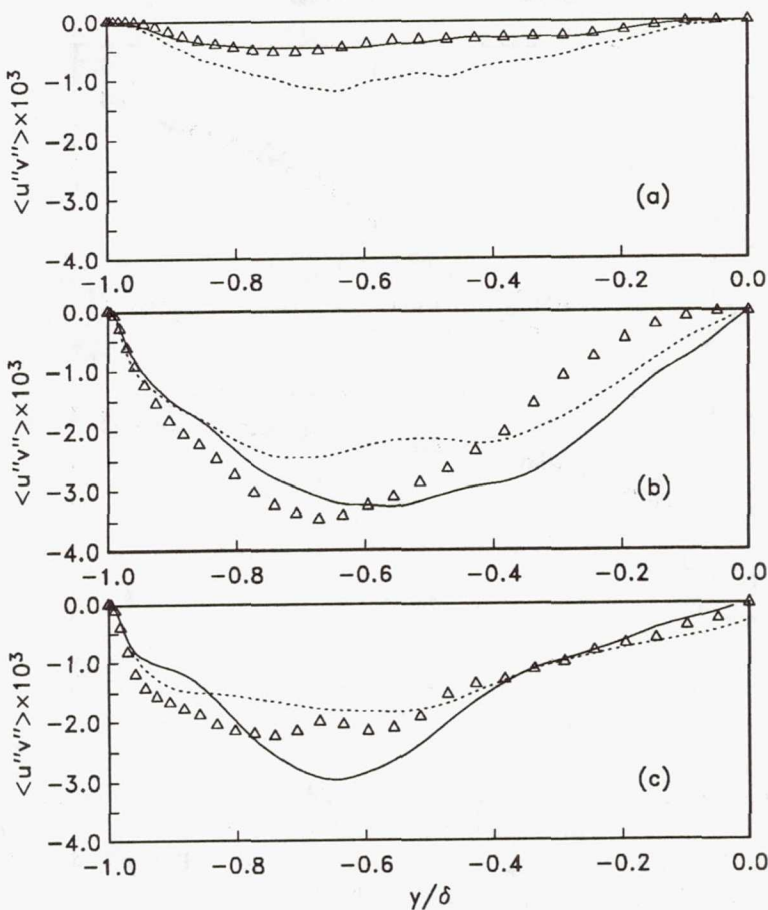


FIGURE 6. Plane-averaged Reynolds stress $\langle u''v'' \rangle$ in transitional channel flow. \triangle Filtered DNS (Zang *et al.* 1990); — present calculation; LES results of Piomelli & Zang (1990b). (a) $t = 176$; (b) $t = 200$; (c) $t = 220$.

collocation method (Zang & Hussaini 1987). The ratio $\alpha = 2$ was chosen. At the initial stages $8 \times 49 \times 8$ grid points were used; the mesh was then progressively refined up to $48 \times 65 \times 64$ points; the dimensions of the computational domain were $2\pi\delta$ in the streamwise direction, and $4\pi\delta/3$ in the spanwise direction. Periodic boundary conditions were applied in the streamwise and spanwise directions; no-slip conditions were applied at the walls.

The time development of the mean wall shear stress $\langle \tau_w \rangle$ is compared in Figure 4 with the DNS results of Zang, Gilbert & Kleiser (1990) and with the results of the LES of Piomelli & Zang (1990b), which used a Smagorinsky model including

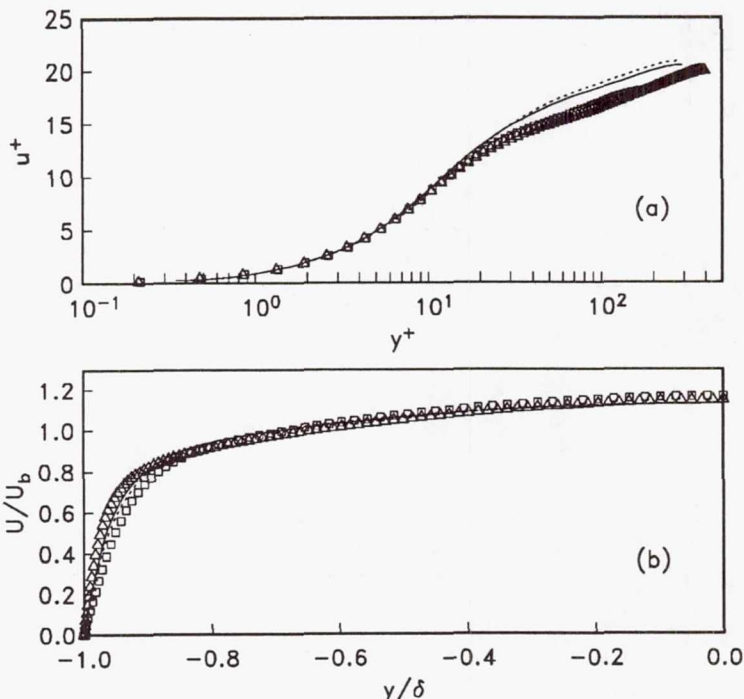


FIGURE 7. Mean velocity profile in fully developed turbulent channel flow. \triangle $Re_\tau = 395$ Filtered DNS (Kim et al. 1987); \square $Re_\tau = 180$ filtered DNS (Kim et al. 1987); — present calculation ($Re_\tau = 295$); LES results of Piomelli & Zang (1990b) ($Re_\tau = 293$). (a) Global coordinates; (b) wall coordinates.

Van Driest damping and an *ad hoc* intermittency function; the present results compare very well with the finely resolved DNS. A coarse direct simulation which can adequately resolve the early stages of transition (up to $t \simeq 170$) cannot predict the drag crisis and the breakdown process with any accuracy (Piomelli & Zang 1990b). The root-mean-square fluctuation of $\langle u''^2 \rangle^{1/2}$ (where $u''_i = \bar{u}_i - \langle \bar{u}_i \rangle$) and the Reynolds shear stress $\langle u'' v'' \rangle$, shown in Figures 5 and 6, are in fair agreement with the DNS results. The DNS results have been filtered using the same filter employed in the LES calculation. Discrepancies between the LES and DNS results at late stages of transition may be due to the fact that, at these times, slight differences in the prediction of the onset of transition may result in significant differences in the instantaneous fields. The capability of the model to predict average backscatter is evidenced by the fact that for $t \leq 185$ the eddy viscosity was negative for significant regions of the channel.

Once fully developed turbulent flow was achieved, statistics were accumulated.

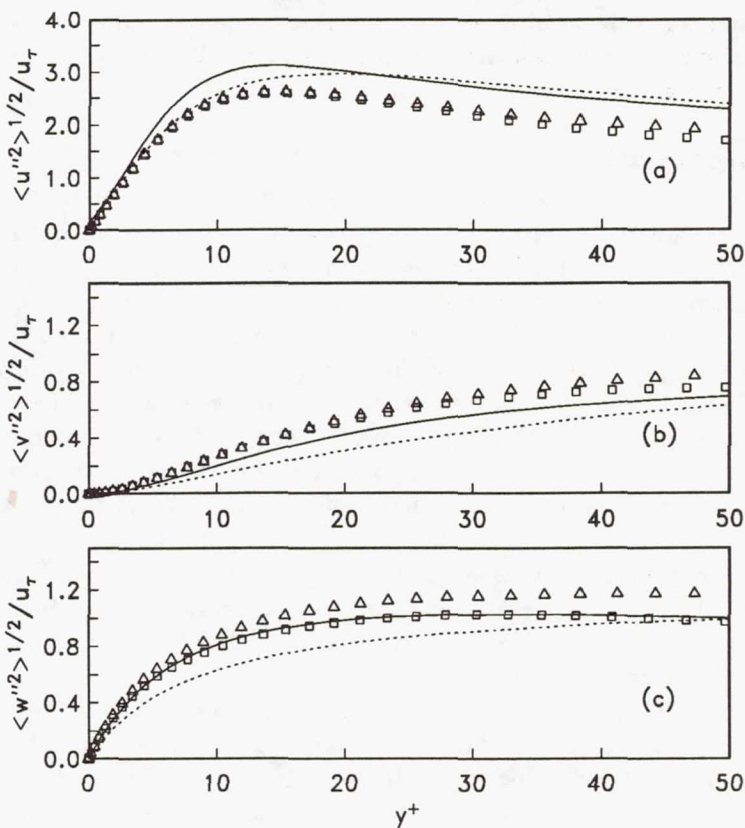


FIGURE 8. Turbulence intensities $\langle u_i''^2 \rangle^{1/2}$ in fully developed turbulent channel flow. \triangle $Re_\tau = 395$ Filtered DNS (Kim *et al.* 1987); \square $Re_\tau = 180$ filtered DNS (Kim *et al.* 1987); — present calculation ($Re_\tau = 295$); LES results of Piomelli & Zang (1990b) ($Re_\tau = 293$). (a) u ; (b) v , (c) w .

The Reynolds number of the turbulent flow was $Re_\tau = 295$ based on friction velocity u_τ and channel halfwidth. The mean velocity profile is shown in Figure 7, normalized by the friction velocity u_τ and by the bulk velocity U_b

$$U_b = \frac{1}{2\delta} \int_{-\delta}^{\delta} \langle \bar{u} \rangle dy. \quad (18)$$

Although an inadequate resolution of the wall layer results in a low value of wall stress, which is reflected in a high value of the intercept of the logarithmic layer in Figure 7b, agreement of the LES results with the DNS data is fairly good. The turbulence intensities $\langle u_i''^2 \rangle^{1/2}$ normalized by the friction velocity u_τ are shown in Figure 8. The DNS results have been filtered using the same filter employed in the LES calculation. In general, the dynamic model gives more accurate results than the Smagorinsky model used by Piomelli & Zang (1990b). The peak of the

streamwise turbulent kinetic energy occurs near $y^+ = 12$, a value also obtained by experiments and numerical simulations; the mean streak spacing was found to be $\lambda^+ = 140$, somewhat larger than the established value of 100, which is also expected of large-eddy simulations.

4. Concluding remarks

A new eddy viscosity subgrid-scale stress model has been presented in which the smallest resolved scales are dynamically tested to predict the behavior of the subgrid scales. This model is based on the algebraic identity (10) between the resolved turbulent stresses and the subgrid-scale stresses obtained using two filters, the grid filter and the test filter. The model coefficient was obtained dynamically as the calculations progress. This procedure exploits the spectral information on the energy content of the smallest resolved scales provided by LES calculations to dynamically adjust the model. The only input to the model is the ratio of test filter width to grid filter width, which was optimized using a numerical turbulent channel flow database. Among the useful properties of the model is its proper asymptotic behavior near the wall without the use of *ad hoc* damping functions.

Large-eddy simulations of transitional and fully developed turbulent channel flow were also carried out. The results were in good agreement with those of direct simulations, and better than those of LES that used the Smagorinsky model with *ad hoc* damping and intermittency functions.

Investigation of the properties of this model when the box filter is employed is desirable. The robustness of the choice $\alpha = 2$ should also be examined by applying the model to flow configurations much different from those studied here. Finally, the use of local space and time averages instead of the plane average used to obtain (16) should be attempted.

REFERENCES

- DEARDORFF, J.W. 1970 A numerical study of three-dimensional turbulent channel flow at large Reynolds numbers. *J. Fluid Mech.* **41**, 453–480.
- GERMANO, M. 1990 Averaging invariance of the turbulent equations and similar subgrid-scale modeling. *CTR Manuscript 116*.
- KIM, J., MOIN, P. & MOSER, R. 1987 Turbulence statistics in fully developed channel flow at low Reynolds number. *J. Fluid Mech.* **177**, 133–166.
- LILLY, D.K. 1966 On the application of the eddy viscosity concept in the inertial sub-range of turbulence. *NCAR Manuscript 123*.
- MASON, P.J. & CALLEN, N.S. 1986 On the magnitude of the subgrid-scale eddy coefficient in large-eddy simulation of turbulent channel flow. *J. Fluid Mech.* **162**, 439–462.
- McMILLAN, O.J., FERZIGER, J.H. & ROGALLO, R.S. 1980 Tests of new subgrid-scale models in strained turbulence. *AIAA Paper No. 80-1339*.

- MOIN, P. & KIM, J. 1982 Numerical investigation of turbulent channel flow. *J. Fluid Mech.* **118**, 341–377.
- PIOMELLI, U., MOIN, P. & FERZIGER, J.H. 1988 Model consistency in large eddy simulation of turbulent channel flows. *Phys. Fluids* **31**(7), 1884–1891.
- PIOMELLI, U., ZANG, T.A., SPEZIALE C.G. & HUSSAINI, M.Y. 1990a On the large-eddy simulation of transitional wall-bounded flows. *Phys. Fluids A* **2**(2), 257–265.
- PIOMELLI, U. & ZANG, T.A. 1990b Large-eddy simulation of transitional channel flow. *1st IMACS Conf. on Computational Physics*, Boulder, June 1990.
- PIOMELLI, U., CABOT, W.H., MOIN, P. & LEE, S. 1990c Subgrid-scale backscatter in transitional and turbulent flows. This volume.
- SMAGORINSKY, J. 1963 General circulation experiments with the primitive equations. I. The basic experiment. *Mon. Weather Rev.* **91**, 99–164.
- VAN DRIEST, E.R. 1956 On the turbulent flow near a wall. *J. Aero. Sci.* **23**, 1007–1011.
- YAKHOT, A., ORSZAG, S.A., YAKHOT, V. & ISRAELI, M. 1989 Renormalization Group formulation of large-eddy simulations. *J. Sci. Comput.* **4**, 139–158.
- YAKHOT, V. & ORSZAG, S.A. 1986 Renormalization Group analysis of turbulence. *J. Sci. Comput.* **1**, 3–51.
- ZANG, T.A. & HUSSAINI, M.Y. 1987 Numerical simulation of nonlinear interactions in channel and boundary-layer transition. In *Nonlinear wave interactions in fluids*, R.W. Miksad, T.R. Akylas and T. Herbert, eds., ASME, New York, 131–145.
- ZANG, T.A., GILBERT, N. & KLEISER, L. 1990 Direct numerical simulation of the transitional zone. In *Instability and transition*, M.Y. Hussaini and R.G. Voigt eds., Springer-Verlag, New York, 283–299.